Journal of the European Ceramic Society 43 (2023) 462–467

Contents lists available at ScienceDirect

Journal of the European Ceramic Society

journal homepage: www.elsevier.com/locate/jeurceramsoc

Surface kinetics and bulk transport in $La_2Ni_{0.5}Cu_{0.5}O_{4+\delta}$ membranes from conductivity relaxation

Zuoan Li [a,b], Reidar Haugsrud [a,*]

[a] University of Oslo, Department of Chemistry, Centre for Materials Science and Nanotechnology, FERMiO, Gaustadalleen 21, NO-0349 Oslo, Norway
[b] SINTEF Industry, Sustainable Energy Technology, Pb. 124 Blindern, NO-0314 Oslo, Norway

ARTICLE INFO

Keywords:
Conductivity relaxation
Surface modification
Surface exchange mechanisms
Oxygen diffusion
La2Ni0.5Cu 0.5 $O_{4+\delta}$
$La_2NiO_{4+\delta}$

ABSTRACT

This work reports conductivity relaxation measurements on both uncoated (1.2 mm thick) and coated (2.0 mm thick) $La_2Ni_{0.5}Cu_{0.5}O_{4+\delta}$ membranes in the temperature range between 550 and 850 °C and oxygen partial pressures from 0.01 to 1.0 atm. The results show that surface kinetics has a significant effect on the relaxation profiles, especially at low temperatures and should not be neglected when extracting transport parameters. Oxygen chemical diffusion and surface exchange coefficients have been determined by transient conductivity with surface modification. Higher activation energy of surface exchange compared to bulk diffusion is observed for $La_2Ni_{0.5}Cu_{0.5}O_{4+\delta}$, similar to that for $La_2NiO_{4+\delta}$. Based on the oxygen partial pressure dependence of the surface exchange coefficient, it has been revealed that oxygen dissociative adsorption rate-limits the surface exchange.

1. Introduction

As a mixed oxide ion and electron conductor, $La_2NiO_{4+\delta}$ has attracted interest due to potential applications as cathode materials for intermediate temperature solid oxide fuel cells (SOFCs), membranes for oxygen separation and reactors, and catalysts for chemical production [1–8].

Large-scale application of $La_2NiO_{4+\delta}$ membranes requires fabrication of dense, thin films, and powders of the material must therefore have good sinterability. Consequently, strategies to improve sinterability without deteriorating the catalytic activity and transport properties are pursued. A-site doping with Sr has shown to increase the electronic conductivity, but decreases oxygen diffusivity [5]. Moreover, Sr substitution leads to Sr segregation to the surface of lanthanum nickelate affecting the catalytic activity [9,10]. Substitution of moderate amounts of Cu for Ni has shown improved sinterability and decrease in ASR without significant effect on the oxygen diffusivity [4,11–13]. However, for surface kinetics of Cu-substituted $La_2NiO_{4+\delta}$, conflicting results have been reported. Flux measurements have shown that surface exchange limits oxygen permeation of $La_2Ni_{0.8}Cu_{0.2}O_{4+\delta}$ membranes with thicknesses of 0.6 and 1.0 mm at temperatures below 973 °C [14]. The effect of temperature on the processes limiting the flux reflects the higher activation energy of surface exchange compared to that of bulk diffusion for these nickelates [1,3,5,11]. When interpreting electrical conductivity relaxation (ECR) measurements, it has, on the other hand, been assumed that relaxation is diffusion controlled for $La_2Ni_{0.5}Cu_{0.5}O_{4+\delta}$ samples with thicknesses of 1.3 and 0.7 mm, even at low temperatures, e.g. 500 °C [15]. ECR requires a small step change in oxygen chemical potential in order to ensure linear surface exchange kinetics and extract chemical diffusion and surface exchange coefficients through either oxidation or reduction [16,17]. Thus, measurements of oxygen surface kinetics of Cu-substituted $La_2NiO_{4+\delta}$ with careful experimental design are called for to clarify these contradicting reports.

In a previous work [18], we have, by using surface coatings of nano-particles of the membrane material, converted a relaxation process originally influenced by both surface exchange and diffusion to solely diffusion control. Similar strategy was also reported by Egger et al. by coating a thin layer (200 nm) of Ag [19] and by Na et al. by coating a porous $(La_{0.6}Sr_{0.4})_{0.95}Co_{0.2}Fe_{0.8}O_{3-\delta}$ (LSCF) on LSCF disc [20]. This simplifies the determination of the kinetic parameters and avoids multiple correlated solutions, as often observed for mixed relaxation processes [21]. A conductivity setup was developed with pressure changes in a high-pressure cell to achieve fast gas exchange close to the sample during the measurement [18]. In this work, the same strategy will be applied to $La_2Ni_{0.5}Cu_{0.5}O_{4+\delta}$ to reveal whether surface exchange limits the relaxation process, and to extract both oxygen surface exchange and

* Corresponding author.
E-mail address: reidar.haugsrud@kjemi.uio.no (R. Haugsrud).

https://doi.org/10.1016/j.jeurceramsoc.2022.10.046
Received 6 July 2022; Received in revised form 10 October 2022; Accepted 17 October 2022
Available online 19 October 2022

diffusion coefficients. Oxygen surface exchange mechanisms and the overall rate determining step (rds) will be discussed based on oxygen partial pressure dependence of the surface exchange coefficients.

2. Experimental

Powders of $La_2Ni_{0.5}Cu_{0.5}O_{4+\delta}$ were synthesized through a citrate-nitrate route. First, La_2O_3 (Unocal Molycorp, 99.99%) was dried at 1100 °C for 3 h, weighed, and dissolved in dilute HNO_3 before stoichiometric amounts of $Ni(NO_3)_2{\cdot}(H_2O)_6$ (Strem Chemicals, 99.9 + %) and $Cu(NO_3)_2 \bullet 2.5(H_2O)$ (Aldrich, 99.99 + %) were added. Then, citric acid (VWR, 99.99 + %) was added in a molar ratio of 1:1 with respect to the total amount of metal nitrates. The solution was dried on a hot plate under constant stirring until a viscous gel was formed. Upon further heating, auto-ignition of the gel took place producing fine grained powders. The resin was fired at 500 °C for 2 h to remove organic residues and then calcined at 1000 °C for 5 h. After the calcination, X-ray diffraction (XRD) confirmed that the product was single-phase, tetragonal $La_2NiO_{4+\delta}$ with the K_2NiF_4 structure.

The as-synthesized powder was uniaxially pressed into disks, 25 mm in diameter, at ~120 MPa and sintered in ambient air at 1300 °C for 3 h. The relative density became higher than 95%, as shown in Fig. 1 by SEM images of the surface and cross section of a sintered sample. The grain size after sintering is around 2 μm. Two sintered tablets were polished with diamond abrasive down to 1 μm yielding final thicknesses of 1.2 and 2.0 mm. The 1.2 mm thick sample was first used for conductivity relaxation measurements (denoted as the 'uncoated sample'), meanwhile the 2.0 mm thick sample was modified by a surface coating procedure ('coated sample') prior to conductivity relaxation measurements. Calcined $La_2Ni_{0.5}Cu_{0.5}O_{4+\delta}$ fine grained powder (200–400 nm in diameter) was dispersed in a mixture of 2% polyvinylpyrolidon (Fluka Ag, Buchs SG) and isopropanol. The resulting slurry was loaded into the air-spray gun (Paasche air brush system) with a continuous supply of high pressurized air to aid the coating process. After coating, the sample was annealed at 1200 °C for 1 h to form thin porous layers on both sides.

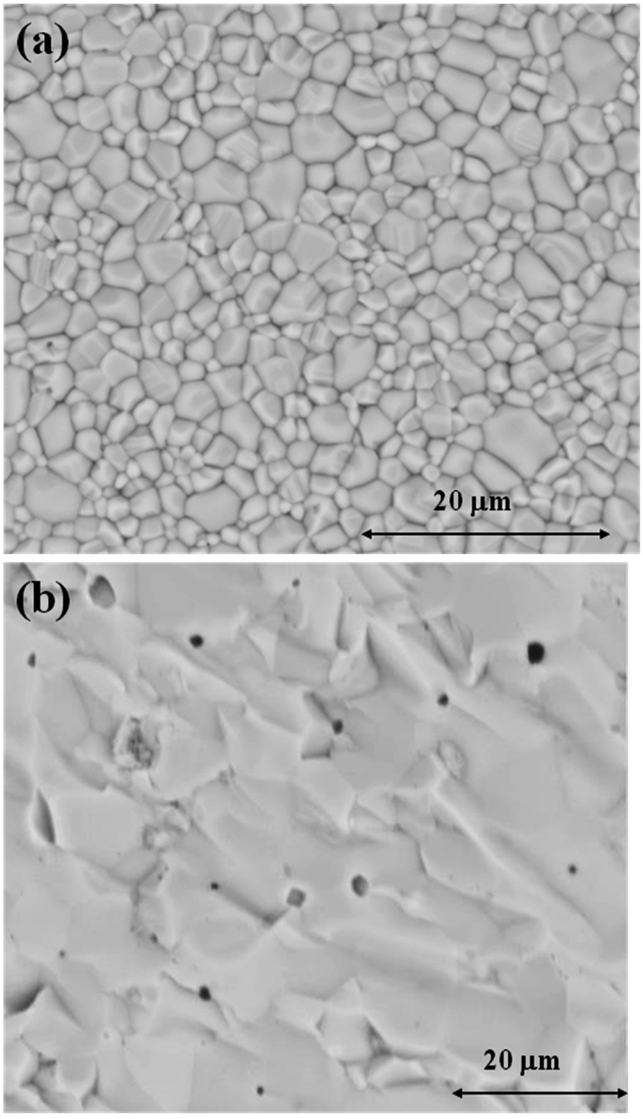

Fig. 1. Sample surface (a) and cross section (b) of $La_2Ni_{0.5}Cu_{0.5}O_{4+\delta}$ after sintering at 1300 °C for 3 h.

The conductivity relaxation measurements were performed in the temperature range of 550–850 °C and oxygen partial pressures from 0.01 to 1.0 atm for both uncoated and coated samples. The total conductivity was measured by the four-point dc (van der Pauw) method [22] using an HP 34420 A Nano Volt / Micro Ohm Meter. To obtain fast gas exchange in the conductivity cell, a high-pressure version of ProboStat (up to 20 bars, NorECs, Norway) was connected directly to a bottle of compressed synthetic air and a rotary pump. The oxidation process was realized by letting compressed air into the cell, while the reduction was done by releasing gas from the cell or pumping the cell. To assume constant transport parameters, the ratio between the initial and the final pO_2 was in the range of 0.1–1 atm during all the measurements. The detailed experimental setup can be found elsewhere [11].

3. Mathematics of oxygen chemical relaxation

When the oxygen partial pressure surrounding a mixed oxide ion electron conductor is changed abruptly, the oxygen stoichiometry of the sample will change to re-establish thermodynamic equilibrium between the gas phase and the oxide. This relaxation process involves surface exchange and bulk diffusion of oxygen species and can be monitored by changes in conductivity. For a plane sheet model, the analytical solution for the conductivity relaxation can be expressed as [23].

$$\frac{\sigma(t)-\sigma(0)}{\sigma(\infty)-\sigma(0)} = 1 - \sum_{n=1}^{\infty} \frac{2A^2 \exp\left(-\beta_n^2 D_{\text{chem}} t/l^2\right)}{\beta_n^2\left(\beta_n^2 + A^2 + A\right)} \tag{1}$$

where σ(0), σ(*t*), and σ(∞) denote the conductivity at the initial time, time *t*, and infinite time, respectively, and D_{chem} is the chemical diffusion coefficient of oxygen. *A* is a measure of the contribution from the surface exchange and defined as the ratio of half the sample thickness *l* to the characteristic length l_d,

$$A = \frac{l}{l_d} = \frac{l \times k_{\text{chem}}}{D_{\text{chem}}} \tag{2}$$

The coefficients, β_n, in Eq. (1) are the positive roots of the so-called transcendental equation

$$\beta_n \tan \beta_n = A \tag{3}$$

which can be solved numerically [24].

For the two limiting cases for conductivity relaxation, when either surface or bulk kinetics predominates, Eq. (1) simplifies to:

i) For a surface exchange-controlled process:

$$\frac{\sigma(t)-\sigma(0)}{\sigma(\infty)-\sigma(0)} = 1 - \exp\left(\frac{-k_{\text{chem}} t}{l}\right) \tag{4}$$

ii) For a diffusion-controlled process:

$$\frac{\sigma(t)-\sigma(0)}{\sigma(\infty)-\sigma(0)} = 1 - \sum_{n=0}^{\infty} \frac{8}{(2n+1)^2\pi^2} \exp\left[\frac{-(2n+1)^2\pi^2 \widetilde{D} t}{4l^2}\right] \tag{5}$$

4. Results and discussion

4.1. Surface coating vs. relaxation patterns

Fig. 2 compares the relaxation profiles at 600 °C upon changing pO_2 from 1.0 to 0.2 atm for 2.0 mm and 1.2 mm thick $La_2Ni_{0.5}Cu_{0.5}O_{4+\delta}$ specimens, coated and uncoated, respectively. For the uncoated, thiner sample, it takes more than 5000 s to reach equilibrium, while shorter time is needed (~2000 s) for the coated, thicker one. This demonstrates considerable enhancement of the surface kinetics by coating powder of the same material onto the surfaces. Nevertheless, the surface kinetics was discarded for conductivity relaxations of 1.3 mm and 0.7 mm samples reported in Ref. [15]. When the temperature is increased to 850 °C, it takes as shown in Fig. 3, on the other hand, longer time to reach equilibrium for the coated sample than for the uncoated one. This indicates that diffusion influences the relaxation more strongly than surface exchange at higher temperature reflecting higher activation energy of surface exchange compared to that of diffusion. This behaviour is in accordance with reports on $La_2NiO_{4+\delta}$ based on tracer exchange and conductivity relaxation [1,18]. Although the thick sample has been coated with porous layers, the conductivity under equilibrium conditions remains the same as for the uncoated one, presented here as a function of inverse temperature in Fig. 4. Consequently, the coating does not change the bulk diffusion but only the surface kinetics. The total conductivity decreases as temperature increases in the experimental window, which is caused by reduced electron hole concentration with increased temperature [11,14,25].

Eq. (1) has not been used to fit both D_{chem} and k_{chem} simultaneously in this work, since it has been demonstrated [18,21] that multiple correlated solutions (several local minima) resulted from a relaxation profile of mixed surface exchange and diffusion control. Here, the measured relaxation data at 600 °C (c.f. Fig. 2) has been taken as an example to show the fitting procedure. Since the coating enhances the surface kinetics significantly, we can treat the transient process for the coated sample as diffusion controlled. This is demonstrated in Fig. 5 by the agreement between the fit based on Eq. 5 (black, dashed lines) and the measured data points. We can, accordingly derive D_{chem} by this approach. As demonstrated, the coating only changes surface kinetics and D_{chem} should therefore be identical for both samples. By fixing D_{chem} in the full solution, k_{chem} for the uncoated thin sample can be extracted through Eq. (1), which yields $D_{chem} = 5.3 \times 10^{-6}$ cm^2/s and $k_{chem} = 5.8 \times 10^{-5}$ cm/s at 600 °C. The reproducibility of the full solution fitting in Fig. 5 confirms, in turn, that D_{chem} extracted from surface coating data is reliable, particularly considering the different thicknesses for two samples. Similarly, D_{chem} has been derived from the relaxation data for the coated, thick sample, and the corresponding k_{chem} has thereafter been determined from the transient of the uncoated sample.

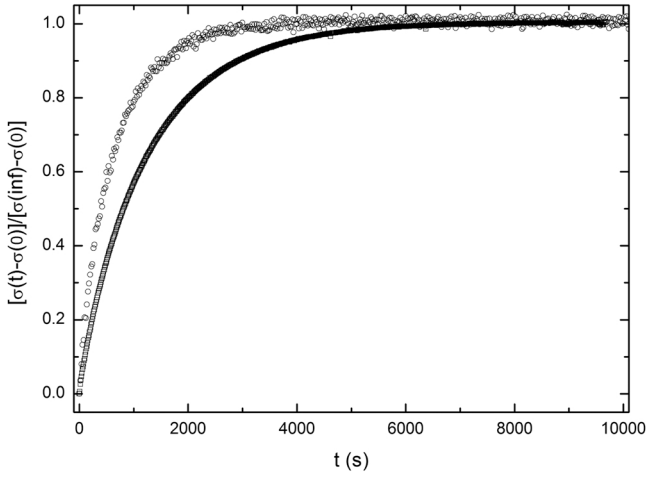

Fig. 2. Normalized conductivity of $La_2Ni_{0.5}Cu_{0.5}O_{4+\delta}$ vs. time at 600 °C upon a step change in pO_2 from 1.0 to 0.2 atm for the coated, thick (○) and uncoated, thin (□) samples.

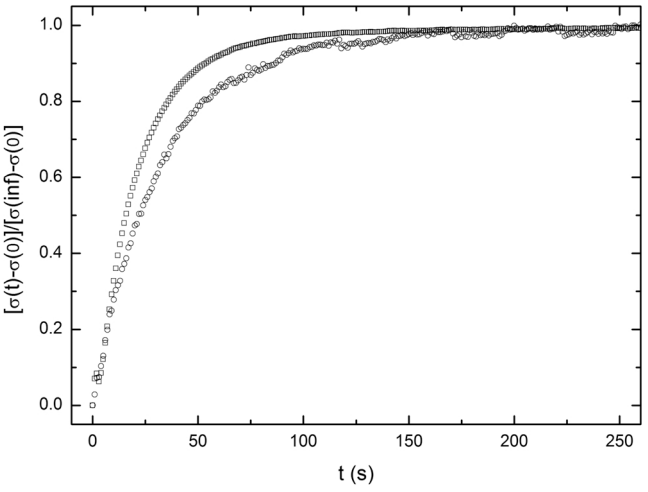

Fig. 3. Normalized conductivity of $La_2Ni_{0.5}Cu_{0.5}O_{4+\delta}$ vs. time at 850 °C upon a step change in pO_2 from 1.0 to 0.2 atm for the coated, thick (○) and uncoated, thin (□) samples.

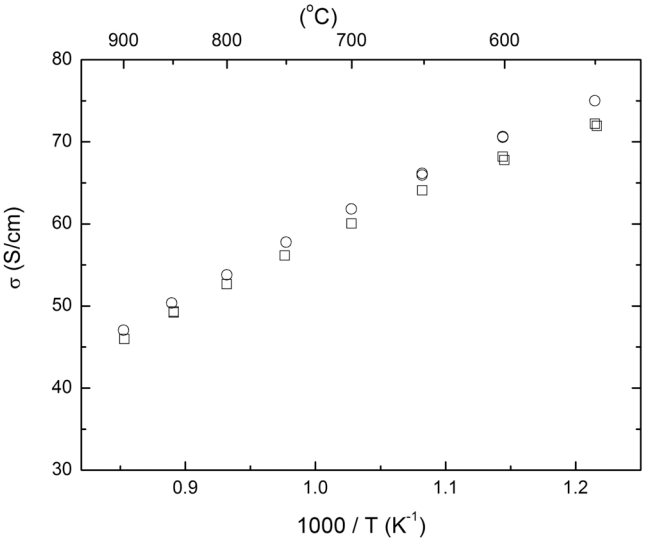

Fig. 4. Conductivity of $La_2Ni_{0.5}Cu_{0.5}O_{4+\delta}$ as a function of inverse absolute temperature at $pO_2 = 0.2$ atm for the uncoated, thin (□) and the coated, thick (○) samples.

We also tried to fit the solution for diffusion controlled behaviour (Eq. 5) to the relaxation data of the uncoated, thin sample at 600 °C which yielded $D_{chem} = 9 \times 10^{-7}$ cm^2/s, approximately a factor of 5 lower than $D_{chem} = 5.3 \times 10^{-6}$ cm^2/s derived from the combined fitting and with poor goodness of fit as demonstrated by the deviation between the model fit (red dashed line) and the data points in Fig. 5. At higher temperatures, the differences in D_{chem} derived from these two approaches are not so significant, supporting the previous observation that surface exchange is enhanced relative to diffusivity at high temperatures: e.g. at 850 °C, 9.7×10^{-5} cm^2/s (combined fitting) vs. 4.8×10^{-5} cm^2/s (diffusion fitting). Thus, extracting diffusivities using Eq. (5) must be done with great caution, especially when surface kinetics cannot be neglected.

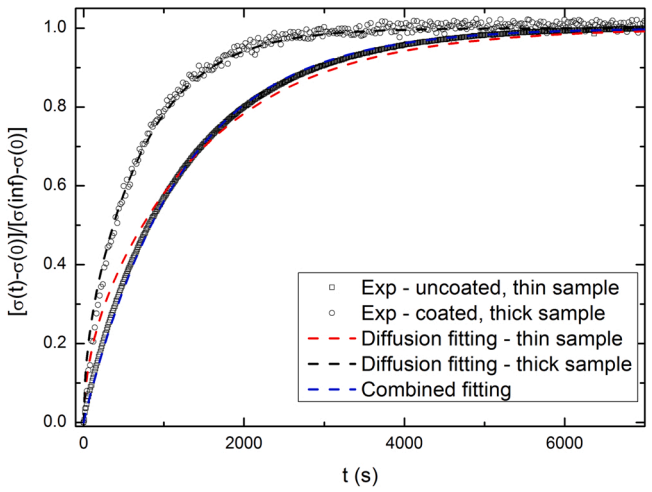

Fig. 5. Fittings by combining the measured relaxation data of the coated, thick (○) and uncoated, thin (□) $La_2Ni_{0.5}Cu_{0.5}O_{4+\delta}$ samples at 600 °C for a step pO_2 change from 1.0 to 0.2 atm. The black, dashed line corresponds to a diffusion controlled fitting based on Eq. 5 (D_{chem} = 5.3 ×10^{-6} cm^2/s), and the blue, dashed line represents a full solution fitting according to Eq. 1 (k_{chem} = 5.8 ×10^{-5} cm/s) while D_{chem} was fixed to 5.3 × 10^{-6} cm^2/s during the fitting. The red, dashed line stands for fitted results using Eq. 5 for the uncoated, thin sample with D_{chem} = 9 × 10^{-7} cm^2/s.

4.2. Bulk diffusion

Based on the above analyses, oxygen chemical diffusion coefficients of $La_2Ni_{0.5}Cu_{0.5}O_{4+\delta}$ were extracted from the relaxation data of the coated, thick sample. Fig. 6 presents pO_2-dependence of D_{chem} in the temperature range of 700–850 °C. A linear behaviour is encountered within the experimental window, and the slope is close to 1/6, reflecting that doubly charged oxygen interstitials are charge-compensated by electron holes [1–3].

$$\frac{1}{2}O_2(g) = O''_i + 2h^{\cdot} \quad (6)$$

This oxygen pressure dependence shows that the substitution with Cu does not change the defect situation for oxygen transport.

Fig. 7 presents diffusion coefficients as a function of the inverse absolute temperature, from both oxidation (pO_2 change from 0.2 to 1.0 atm) and reduction (pO_2 change from 1.0 to 0.2 atm) transients. The higher final oxygen partial pressure yields higher oxygen chemical

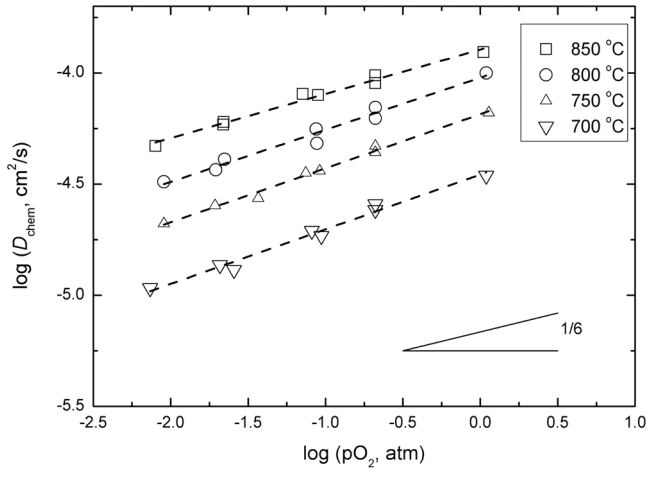

Fig. 6. Double-log plot of D_{chem} vs. pO_2 in $La_2Ni_{0.5}Cu_{0.5}O_{4+\delta}$ at various temperatures. The dashed lines are linear-fittings of the experimental data at each temperature marked in the plot.

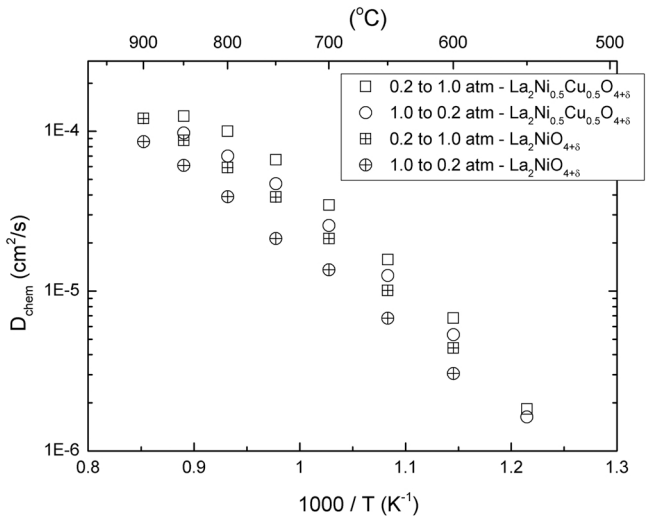

Fig. 7. Temperature dependence of D_{chem} in $La_2Ni_{0.5}Cu_{0.5}O_{4+\delta}$ in comparison with those of the undoped [18].

diffusion coefficients as a result of increased concentration of oxygen interstitials [3]. Cu substitution on Ni sites do, under sufficiently oxidizing conditions, not require charge compensation. Upon substitution, the electron hole and the oxygen interstitial concentration might slightly decrease. However, the Cu-substitution leads to a slight increase in the oxygen diffusivity as compared to undoped $La_2NiO_{4+\delta}$, in contrast to Sr-doping where the chemical diffusion coefficients have been reported to decrease [1,5]. It can be seen from Fig. 7 that D_{chem} follows an Arrhenius-type behaviour at each pO_2 with similar activation energy of ~107 ± 7 kJ/mol, relatively close to that reported for the undoped $La_2NiO_{4+\delta}$, ~90 kJ/mol [1,18]. Considering relatively large grain size (~2 μm) of sintered $La_2Cu_{0.5}Ni_{0.5}O_{4+\delta}$, the grain boundary effect should not influence bulk diffusivity while the undoped $La_2NiO_{4+\delta}$ might have an enhanced grain boundary effect due to lower activation energy.

For mixed ionic electronic conductors where t_{el}~1, the oxygen chemical and self diffusion coefficients are related through [26].

$$D_{chem} \approx wD_O = \frac{1}{2} \times \frac{\partial \ln(pO_2)}{\partial \ln(c_o)} D_o \quad (7)$$

where w is the so-called thermodynamic factor and can be determined experimentally by thermogravimetry. The oxygen tracer and self diffusion coefficients are related through $D^* = f \cdot D_O$, where f is the correlation factor and assumed to be unity for migration via an interstitial mechanism [27]. The thermodynamic factors in the temperature range of 500–900 °C were taken from Ref. [15]. Since oxygen in nickelates migrates via the interstitial mechanism, we can use the tracer diffusion coefficients of $La_2Cu_{0.5}Ni_{0.5}O_{4+\delta}$ [2,15] and $La_2NiO_{4+\delta}$ directly [1], and calculate the wD^* products. The calculated data and the experimentally determined D_{chem} from the present investigation are compared in Fig. 8 (including the original tracer diffusion data). The consistency for $La_2Cu_{0.5}Ni_{0.5}O_{4+\delta}$ among different techniques and comparable results with the undoped $La_2NiO_{4+\delta}$ are acceptable. This also supports the current methodology for determining more accurate oxygen chemical diffusion coefficients.

4.3. Surface exchange

k_{chem} was extracted by fitting Eq. (1) to the relaxation data of the uncoated sample and the calculated values of k_{chem} in $La_2Ni_{0.5}Cu_{0.5}O_{4+\delta}$ are plotted in Fig. 9 as a function of inverse absolute temperature, in addition to those of $La_2NiO_{4+\delta}$ for comparison [18]. The product of wk^* of $La_2Ni_{0.5}Cu_{0.5}O_{4+\delta}$ [2] is included in Fig. 9, deviating significantly from the present data set. This might be due to scattered original tracer

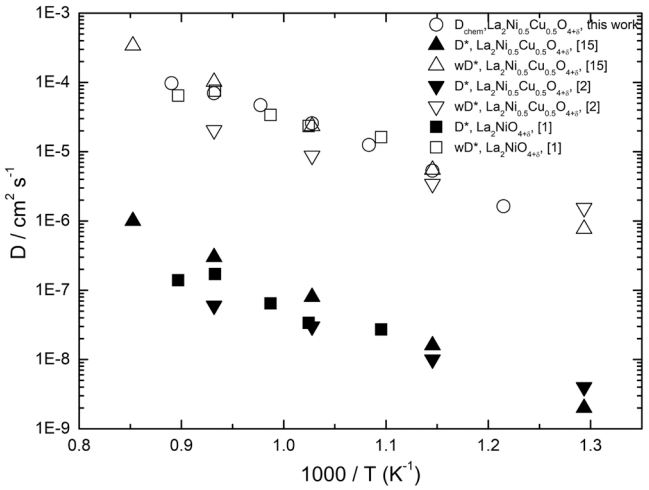

Fig. 8. Comparison of D_{chem}, D* and wD*in $La_2Ni_{0.5}Cu_{0.5}O_{4+\delta}$ [2,15] and $La_2NiO_{4+\delta}$ [1] as a function of inverse temperature.

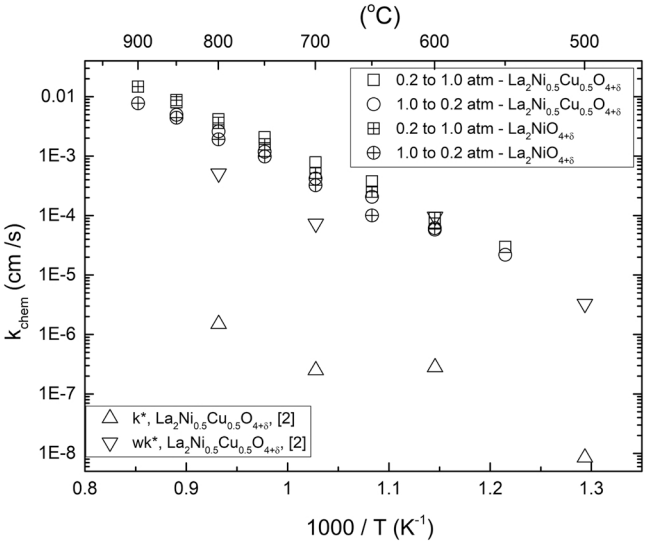

Fig. 9. Temperature dependence of k_{chem} in $La_2Ni_{0.5}Cu_{0.5}O_{4+\delta}$ from this work and $La_2NiO_{4+\delta}$ from Ref. [18], and k * and wk* of $La_2Ni_{0.5}Cu_{0.5}O_{4+\delta}$ [2].

exchange data. It is also clear from Fig. 9 that the Cu-substitution does not change significantly k_{chem} compared to values for the nominally undoped material. The data follow Arrhenius-type behaviour with activation energies of 147 ± 5 kJ/mol at 1.0 atm and 141 ± 3 kJ/mol at 0.2 atm, again well in accordance with those of the undoped $La_2NiO_{4+\delta}$: 1.61 eV (155 kJ/mol) from tracer exchange [1] and ~150 kJ/mol from conductivity relaxation measurements [18].

The measured k_{chem} is a lumped parameter and includes a series of reaction steps, e.g., oxygen adsorption, dissociation, charge transfer, and oxygen incorporation etc. To study surface exchange mechanisms and determine possible rate determining steps (rds) in $La_2Ni_{0.5}Cu_{0.5}O_{4+\delta}$, the pO_2-dependence of k_{chem} has been measured at several temperatures as presented in Fig. 10. The functional dependence is essentially constant with a slope of ½ in the double-logarithmic plot of k_{chem} vs. pO_2. To simplify the possible surface exchange mechanism, we only consider oxygen dissociation and incorporation as follows

$$\frac{1}{2}O_2(g) \leftrightarrow O'_{ad} + h^{\cdot} \tag{8}$$

$$O'_{ad} + V^{\cdot\cdot}_{o,s} \leftrightarrow O^{\times}_{o,s} + h^{\cdot} \tag{9}$$

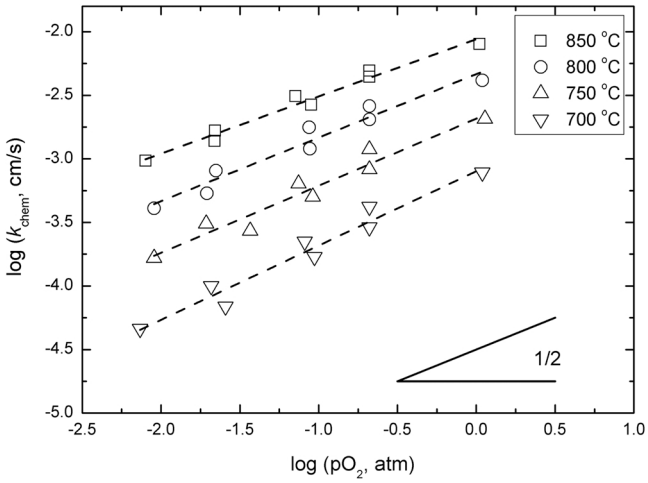

Fig. 10. Double-log plot of k_{chem} vs. pO_2 in $La_2Ni_{0.5}Cu_{0.5}O_{4+\delta}$ at various temperatures. The dashed lines are linear-fittings of the experimental data at each temperature marked in the plot.

For direct oxygen dissociation, it requires more than 5 eV to break an oxygen bond, while much lower energy is needed for charged oxygen species [28]. Therefore, we treat charge transfer and oxygen dissociation together in Reaction 8. According to Maier [29], chemical kinetics can be applied to derive an atomistic expression for the surface exchange by assuming that one step in the pathway is rate determining and all pre- and succeeding steps are under quasi-equilibrium. If Reaction 8 is rate determining, one can write the total exchange rate as

$$r = \overrightarrow{k}\, p(O_2)^{1/2} - \overleftarrow{k}\frac{[O_O^{\times}][h^{\cdot}]^2}{K_9[V_o^{\cdot\cdot}]} \tag{10}$$

where $\overrightarrow{k}$ and $\overleftarrow{k}$ are the forward and backward reaction constants of Reaction 8, respectively, and K_9 is the equilibrium constant of the incorporation reaction (9). Since oxygen interstitials and electron holes compensate each other according to Reaction 6, one can obtain

$$[h^{\cdot}], \left[O_i^{//}\right] \propto p(O_2)^{1/6} \tag{11}$$

From literature one finds that the anion Frenkel defects, $V_O^{\bullet\bullet}$ and $O_i^{//}$, are predominating under stoichiometry. Applying the anion Frenkel equation, the concentration of oxygen vacancies can be expressed as

$$[V_o^{\cdot\cdot}] \propto p(O_2)^{-1/6} \tag{12}$$

By inserting Eqs. (11) and (12) into Eq. (10), one can finally express exchange rate as

$$r \propto p(O_2)^{1/2} \tag{13}$$

which is in accordance with the slope shown in Fig. 10. Deriving the pO_2 dependence of other potential rate determining surface reactions, different dependences than ½ are obtained supporting that the surface exchange of $La_2Ni_{0.5}Cu_{0.5}O_{4+\delta}$ is limited by the oxygen dissociative adsorption. Considering that Ni is absent from the surface [10], oxidation of B site cations will be hindered for charge transfer in Reaction 8 so that the oxygen dissociative adsorption will become restrained.

The surface exchange of nominal $La_2NiO_{4+\delta}$ was studied by Bouwmeester et al. [30] using a pulse isotope exchange technique, from which the total exchange rate can be deconvoluted into oxygen dissociative adsorption and incorporation. It was shown that the dissociative adsorption of oxygen rate-limits the total exchange process. The rate determining step suggested also rationalizes the positive effect of coating with porous materials on the surface: By increasing the area of

active surface sites for oxygen adsorption and dissociation, the rate determining step for the surface exchange is overcome and the transient process transforms from being affected by both diffusion and surface exchange to becoming a pure diffusion-controlled relaxation.

All in all, the methodology utilized in this work is adequate to derive reliable kinetic parameters. Since both surface and bulk transport parameters of membranes can be determined, this approach may be applied to derive the gaseous flux through a membrane for a specific thickness of a material [11,31]. Consequently, one may firmly evaluate candidate materials to serve as dense ceramic oxygen gas separation membranes. As thin (micro-scale) membranes are generally required for higher separation efficiency, surface kinetics usually dominates the overall oxygen permeation. With the present methodology, it is also possible to reveal the rate-limiting step for surface processes, and, by this insight, seek to overcome this limit by modifications of the surface, e.g. applying surface coating as in this work.

5. Concluding remarks

Surface modification by coatings and fast changes of the total pressure has been used to aid accurate determination of oxygen diffusivity and oxygen surface exchange coefficients of $La_2Ni_{0.5}Cu_{0.5}O_{4+\delta}$ from conductivity relaxation measurements.

Surface exchange has a significant effect on the total relaxation, especially at low temperatures. Cu-substitution of $La_2NiO_{4+\delta}$ has minor effects on the oxygen chemical diffusion and surface exchange coefficients. The pO_2-dependence of the surface exchange coefficient revealed that oxygen dissociative adsorption rate-limits the oxygen surface exchange on $La_2Ni_{0.5}Cu_{0.5}O_{4+\delta}$. Considering the good sinterability of this material, Cu-substituted $La_2NiO_{4+\delta}$ should be a promising candidate as an oxygen separation membrane.

Declaration of Competing Interest

The authors declare that they have no known competing financial interests or personal relationships that could have appeared to influence the work reported in this paper.

Acknowledgements

Financial support from the Research Council of Norway (RCN) under the project of (KINOXPRO) (RENERGI 190901/S60), FUSKE (262393) and MOC-OTM (268450) is gratefully acknowledged.

References

[1] S.J. Skinner, J.A. Kilner, Solid State Ion. 135 (2000) 709–712.
[2] E. Boehm, J.M. Bassat, M.C. Steil, P. Dordor, F. Mauvy, J.C. Grenier, Solid State Sci. 5 (2003) 973–981.
[3] J.B. Smith, T. Norby, J. Electrochem. Soc. 153 (2006) A233–A238.
[4] A. Aguadero, J.A. Alonso, M.J. Escudero, L. Daza, Solid State Ion. 179 (2008) 393–400.
[5] Z. Li, R. Haugsrud, J.B. Smith, T. Norby, J. Electrochem. Soc. 156 (2009) B1039–B1044.
[6] A.P. Tarutin, J.G. Lyagaeva, D.A. Medvedev, L. Bi, A.A. Yaremchenko, J. Mater. Chem. A 9 (2021) 154–195.
[7] A. Das, E. Xhafa, E. Nikolla, Catal. Today 277 (2016) 214–226.
[8] P.D.K. Nezhad, et al., Appl. Catal. A Gen. 612 (2021), 117984.
[9] M.S.D. Read, M.S. Islam, G.W. Watson, F.E. Hancock, J. Mater. Chem. 11 (2001) 2597–2602.
[10] J. Wu, S.S. Pramana, S.J. Skinner, J.A. Kilnera, A.P. Horsfield, J. Mater. Chem. A 3 (2015) 23760–23767.
[11] Z. Li, T. Norby, R. Haugsrud, J. Am. Ceram. Soc. 95 (2012) 2065–2073.
[12] H. Chen, X. Li, X. Du, H. Xie, L. Zhao, Y. Ling, J. Ceram. Sci. Technol. 9 (2018) 155–162.
[13] M. Ferkhi, S. Khelili, L. Zerroual, A. Ringuede, M. Cassir, Electrochim. Acta 54 (2009) 6341–6346.
[14] V.V. Kharton, E.V. Tsipis, A.A. Yaremchenko, J.R. Frade, Solid State Ion. 166 (2004) 327–337.
[15] F. Mauvy, J.M. Bassat, E. Boehm, P. Dordor, J.P. Loup, Solid State Ion. 158 (2003) 395–407.
[16] J.A. Lane, J.A. Kilner, Solid State Ion. 136–137 (2000) 997–1001.
[17] S. Wang, A. Verma, Y.L. Yang, A.J. Jacobson, Ben Abeles, Solid State Ion. 140 (2001) 125–133.
[18] Z. Li, R. Haugsrud, Solid State Ion. 2016 (2012) 67–71.
[19] A. Egger, W. Sitte, Solid State Ion. 258 (2014) 30–37.
[20] B.T. Na, T. Yang, J. Liu, S. Lee, H. Abernathy, T. Kalapos, G. Hackett, Solid State Ion. 361 (2021) 115561–115569.
[21] R.A. Cox-Galhotra, S. McIntosh, Solid State Ion. 181 (2010) 1429–1436.
[22] H.J.M. Bouwmeester, M.W. den Otter, B.A. Boukamp, J. Solid State Electrochem. 8 (2004) 599–605.
[23] J. Crank, The Mathematics of Diffusion, Clarendon Press, Oxford, 1975, p. 60.
[24] Z. Li, Int. J. Hydrog. Energy 37 (2012) 8118–8122.
[25] J. Song, D. Ning, B. Boukamp, J.M. Bassat, H.J.M. Bouwmeester, J. Mater. Chem. A 8 (2020) 22206–22221.
[26] J. Maier, J. Am. Ceram. Soc. 76 (1993) 1228–1232.
[27] P. Kofstad, Nonstoichiometry, Diffusion and Electrical Conductivity in Binary Metal Oxides, Wiley Interscience, New York, 1972, p. 81.
[28] R. Merkle, J. Maier, Phys. Chem. Chem. Phys. 4 (2002) 890–897.
[29] J. Maier, Solid State Ion. 112 (1998) 197.
[30] H.J.M. Bouwmeester, C. Song, J. Zhu, J. Yi, M. van Sint Annaland, B.A. Boukamp, Phys. Chem. Chem. Phys. 11 (2009) 9640–9643.
[31] H.J.M. Bouwmeester and A.J. Burggraaf, The CRC Handbook of Solid State Electrochemistry (Ed: P.J. Gellings and H.J.M. Bouwmeester), Chapter 14, CRC Press Inc, 1997.